Notes

Viscosimetric, Hydrodynamic, and Conformational Properties of Dendrimers and Dendrons

Brian M. Tande and Norman J. Wagner*

Center for Molecular and Engineering Thermodynamics, Department of Chemical Engineering, University of Delaware, Newark, Delaware 19716

Michael E. Mackay

Department of Chemical Engineering and Material Science, Michigan State University, East Lansing, Michigan 48824

Craig J. Hawker

IBM−Almaden Research Center, 650 Harry Road, San Jose, California 95120

Miyoun Jeong

Department of Chemical, Biochemical and Materials Engineering, Stevens Institute of Technology, Castle Point on the Hudson, Hoboken, New Jersey 07030

Received July 17, 2001
Revised Manuscript Received September 24, 2001

Introduction

Controlling the molecular architecture of dendrimers is crucial for their intended use in applications such as drug delivery, biocides, gene transfer, catalyst supports, and processing aids (see refs 1−3). The molecular conformation in solution and the melt, which will control efficacy in such applications, has been the subject of theory,[4,5] molecular,[6] and coarse-grained simulations[7−11] and extensive experimentation by X-ray, light and neutron scattering,[12−21] and rheology.[12,13,22−27] Of fundamental interest is the location of the terminal groups and molecular density profile as a function of the generation number. Direct, quantitative comparison of theory, experiment, and simulation is often complicated by the various levels of approximation used in the modeling and the need to accurately specify the physical properties of chemical groups and their interactions with the solvent. However, one useful, quantitative indicator of molecular conformation is the ratio of the radius of gyration (R_g) to the viscosimetric radius (R_η) or the hydrodynamic radius (R_h). These ratios can be computed from the molecular architecture without specifying the chemical details and depend primarily on the mass distribution. As such, they are an indication of overall macromolecular geometry and hydrodynamic draining.

The radius of gyration is typically calculated from static scattering measurements, while the hydrodynamic radius (or equivalent sphere radius) is determined by dynamic light scattering or other diffusion measurements. For reference, a solid sphere yields a value of $R_g/R_h = R_g/R_\eta = \sqrt{(3/5)} \approx 0.77$. Core weighting of the density distribution decreases these ratios, and values much higher ($\sim 1.22 \ln(L/D)$, with L/D the aspect ratio) can be achieved by a slender-rod geometry. Larger ratios are generally observed for polymers in solution; the experimental results of Schmidt and Burchard[28] for linear polystyrene and poly(methyl methacrylate) in Θ solvents yield ratios of $R_g/R_h = 1.27$ and 1.16, respectively.

The viscosimetric radius is also an effective hydrodynamic sphere radius but is determined from intrinsic viscosity measurements. Although equal for hard spheres, R_η is generally different from R_h due to the different flow fields generated during the two measurements. The ratio R_g/R_η is inversely related to the Flory−Fox parameter and can be thought of as a measure of how well the molecule is drained by the solvent. Molecules that are easily drained have small viscosimetric radii and Flory−Fox parameters; thus, R_g/R_η becomes large. Using relationships in Flory,[29] the ratio R_g/R_η is calculated as 1.17 for a Gaussian coil in a Θ solvent, based on experimental data for several linear polymers. For highly branched molecules the density of segments is higher than for linear polymers.[30] This results in a larger Flory−Fox parameter (larger R_η) and a smaller value of R_g/R_η. It is expected that these results also depend on the solvent quality; collapsing the polymer in poor solvents should reduce the value toward that of a solid sphere, while expansion of the polymer in good solvents is expected to increase the ratio.

It is clear that these simple comparisons of measurable molecular dimensions can provide valuable information about the conformation of polymers in solution. Here, we extend this idea to explore the effects of extreme branching on polymer conformation, where monodisperse dendrimers of varying generation provide clean model systems for investigation. To begin, we analyze the available experimental and theoretical data in the literature. The two most heavily studied systems are poly(propyleneimine) (PPI) and poly(amidoamine) (PAMAM) dendrimers. We then present new small-angle neutron scattering data for several generations of poly(benzyl ether) *monodendrons* in a good solvent. Comparing this information with previously published intrinsic viscosity results sheds light on the effect of dendritic architecture, solvent quality, and steric crowding on molecular conformation. The new results and the literature results are compared with recent theoretical calculations and simulations of these geometric properties to assess their validity.

Background

The intrinsic viscosity of dendrimers has been the subject of several experimental[12,26,31] and theoretical studies[7,11,32] in an attempt to determine their molecular conformation in solution. Here we focus on the limited

* Corresponding author: e-mail wagner@che.udel.edu.

10.1021/ma011265g CCC: $20.00
Published on Web 10/25/2001

Table 1. Viscosimetric and Hydrodynamic Radii and Radii of Gyration (Å) from Several Experimental Studies of the Intrinsic Viscosity and Self-Diffusion of Poly(propyleneimine) (PPI) Dendrimers; All Data Were Taken at 25 °C

	Bodnar et al.[12] D_2O			Bodnar et al.[12] [a] D_2O			Scherrenberg et al.[18] D_2O			Rietveld[33,42] methanol				
G	R_η	R_g	R_g/R_η	R_η	R_g	R_g/R_η	R_η	R_g	R_g/R_η	R_h	R_η	R_g[b]	R_g/R_h	R_g/R_η
1							6.1	4.4	0.72					
2							8.8	6.9	0.78					
3							11.8	9.3	0.79	12.7	12.1	11.3	0.89	0.93
4	12.7	10.2	0.80	14.7	11.9	0.81	15.6	11.6	0.74	16.5	15.4	13.3	0.81	0.86
5	17.8	14.1	0.79	20.3	16.2	0.80	19.8	13.9	0.70	20.3	19.8	14.3	0.70	0.72

[a] PPI dendrimers with acetylated end groups. [b] R_g values from Prosa et al.[34]

Table 2. Hydrodynamic Radii and Radii of Gyration (Å) from Scattering and Self-Diffusion Studies of Poly(amidoamine) (PAMAM) Dendrimers Containing an Ethylenediamine Core

	Prosa[34] and Stechemesser[36] methanol		
G	R_h[a]	R_g[b]	R_g/R_h
3	19.9	15.8	0.79
4	24.8	17.1	0.68
5			
6	38.2	26.3	0.69
7			
8	57.9	40.3	0.69
9			
10	72.3	57.4	0.79

[a] R_h values from diffusion studies. [b] R_g values from SAXS measurements.

number of studies that measure both R_g and R_η or R_h of dendrimers in solution. Bodnar et al.[13] and Sherrenberg et al.[18] have each studied PPI dendrimers in various solvents to measure both the radius of gyration, R_g, and the viscosimetric radius, R_η. Rietveld and Bedeaux[33] measured the hydrodynamic radius via self-diffusion measurements for PPI in methanol. Another type of dendrimer, poly(amidoamine) (PAMAM), has also been studied by scattering experiments,[34] intrinsic viscosity measurements,[35] and diffusion studies.[36]

The results of these studies are summarized in Tables 1 and 2, showing that for PPI dendrimers these ratios decrease nonmonotonically from 0.93 to 0.70 as the generation number of the dendrimer is varied from one to five. The highest values are obtained for PPI dendrimers in methanol, whereas in a poorer solvent (water), the ratio decreases. For PAMAM dendrimers in methanol, there is not a clear trend, but the values vary between 0.68 and 0.79.

The general trend in the microstructure suggested by these investigations is that dendrimers evolve toward a compact spherical geometry as the generation number is increased. From the experiment results, it can be seen that PPI dendrimers exhibit ratios closer to that of a constant density sphere (≈0.77), which is in general agreement with several detailed analyses of small-angle scattering experiments[12,18,34] and molecular simulations.[12]

For reference, Trollsas et al.,[19] who studied several isomers of dendritic-like star polymers with various branching arrangements, found that R_g/R_h ranged from 0.76 to 0.53, depending strongly on the location of branch points within the molecule. They also concluded that their dendrimer-like star polymers exhibit a compact density distribution, with only slight core or shell weighting.

Two coarse-grained models are available for direct comparison. Mansfield[11] computed the molecular dimensions of dendrimers up to the ninth generation using an on-lattice Monte Carlo method coupled with the angular-averaged hydrodynamic calculation at the Oseen level.[37] Ganazzoli et al.[7] used a self-consistent free energy minimization technique to calculate the equilibrium and dynamic properties of dendrimers in a good solvent. Two types of trifunctional dendrimers were considered; D1 and D2 refer to dendrimers with one or two segments between branch points, respectively. A Zimm-like approach was used to estimate the hydrodynamic interactions. The results from these calculations are shown in Table 3, where it can be seen that the ratio progresses monotonically from a value close to that of a Gaussian coil toward that of a rigid sphere as the generation number increases. The calculations of Ganazzoli et al. yield a more dramatic change with generation and values lower than that for a homogeneous sphere for the highest generations considered. The difference between the viscosimetric and hydrodynamic radii are also greater than those computed by Mansfield. The theoretical values in Table 3 are dimensionless with the segment length.

Comparison of the computed values with the measurements in Tables 1 and 2 demonstrates that both models overestimate the observed ratio of R_g/R_h but do a better job of predicting R_g/R_η. However, experimentally, $R_g/R_\eta > R_g/R_h$; i.e., the viscosimetric radius is smaller than the hydrodynamic radius. Mansfield's calculations yield nearly equal values, while Ganazzoli et al. compute the opposite trend. These predictions also suggest a wide range of conformations, from nearly Gaussian at the lowest generations to compact shell−core structure at the highest generation. The experimental data do not show such dramatic quantitative variation with generation, yet the qualitative structural trend is borne out by the scattering data. It is unclear whether these discrepancies result from assuming incorrect molecular architectures or the approximations used in performing the hydrodynamic calculations.

Experiment

The materials included in this study are single dendrons of poly(benzyl ether) of generation three to six (see Table 4) in two deuterated solvents, benzene (*d*-benzene) and tetrahydrofuran (*d*-THF). The synthesis of these materials has been the subject of a previous paper.[38] A detailed study of the dilute solution properties of these monodendrons in various solvents is the topic of a separate publication.[26]

The small-angle neutron scattering (SANS) measurements were taken using the 30 m NG3 and NG7 SANS instruments at the National Institute for Standards and Technology (NIST) Center for Neutron Research (NCNR) in Gaithersburg, MD. Two instrument configurations were used. The first had five guides, a sample-to-detector distance of 3.8 m, and a 20 cm detector offset, giving a q range of 0.008 51−0.1667 Å^{-1}. The second configuration had five guides, a sample-to-detector distance of 1.0 m, and a 25 cm detector offset, giving a q range

Table 3. Dimensionless Radii from Theoretical Studies of Dendrimers

	Mansfield[11]					Ganazzoli et al.[7] D1					Ganazzoli et al.[7] D2				
G	R_h	R_η	R_g	R_g/R_h	R_g/R_η	R_h	R_η	R_g	R_g/R_h	R_g/R_η	R_h	R_η	R_g	R_g/R_h	R_g/R_η
1	6.4	6.8	7.6	1.19	1.12	0.81	0.99	1.08	1.33	1.09	1.09	1.39	1.45	1.33	1.04
2	9.8	10.2	10.9	1.11	1.06	1.10	1.43	1.37	1.25	0.96	1.49	2.00	1.85	1.25	0.93
3	13.9	14.3	14.2	1.02	0.99	1.39	1.96	1.64	1.18	0.84	1.90	2.74	2.23	1.17	0.81
4	18.8	19.2	17.9	0.95	0.93	1.69	2.61	1.88	1.11	0.72	2.31	3.65	2.58	1.12	0.71
5	24.6	24.9	22.0	0.89	0.88	1.97	3.41	2.11	1.07	0.62	2.70	4.77	2.91	1.08	0.61
6	31.5	31.7	26.8	0.85	0.85	2.22	4.41	2.33	1.04	0.53					
7	39.7	39.8	32.5	0.82	0.82										
8	49.0	49.2	39.0	0.80	0.79										
9	59.7	59.7	46.5	0.78	0.78										

Table 4. Poly(benzyl ether) Monodendrons Investigated in This Study

sample	generation	M_w (Da)	solvents	concn (wt %)
G3	3	1592	*d*-benzene, *d*-THF	5
G4	4	3288	*d*-benzene, *d*-THF	5
G5	5	6687	*d*-benzene, *d*-THF	5
G6	6	13464	*d*-benzene	0.37

of 0.0185−0.5979 Å $^{-1}$. Both configurations used a neutron wavelength of 6 Å with a 15% spread. The samples in *d*-benzene were measured at only the first configuration, while those in *d*-THF were measured at both configurations. All samples were measured at room temperature and at a concentration of 5 wt %, unless noted otherwise.

The raw SANS data sets were reduced to an absolute scale (I (cm^{-1}) vs q (Å)) using the standard NIST procedure. To determine the molecular size, each absolute data set was then analyzed by fitting to both the sphere form factor and the Debye equation (which is used for Gaussian chains) as well as by a Guinier plot. The incoherent background scattering for each sample was determined from an appropriate Porod plot (i.e., Iq^4 vs q^4 for the sphere fits) and incorporated into the fitting procedure. The fit to the sphere scattering equation was found to be superior to the Debye equation, as has been previously observed.[34] The lower range of the scattering vector and the low concentration enabled Guinier plots (i.e., $qR_G \ll 1$). Some samples showed an increase in scattering intensity at low q that is indicative of interparticle interactions or aggregation. For the purposes of this study, the first few points of these curves were excluded from the fitting procedures in order to determine the primary molecular size without including these effects.

The absolute SANS intensity was also used to determine the degree of solvent swelling, assuming the dendron to consist of a sphere of homogeneous scattering length density. This is expressed as the mass fraction of solvent within the equivalent sphere, calculated using a method previously described and employed to analyze PPI dendrimers.[12] The overall scattering length density of the swollen dendrimer is first determined from fitting the absolute SANS intensity. Since the scattering length density of the solvent and dendrimer are known, we can determine the amount of solvent swelling that is necessary to yield the measured overall scattering length density. Assuming partial molar density of the dendrimer to be that of the melt (i.e., ∼1.25 g/cm^3 for the PBE monodendons studied here), these mass fractions can then be used to estimate the degree of nonideality of mixing inside the dendrimer by comparison of the measured molecular radius to that calculated from an assumption of ideal mixing. In all cases, the radius calculated assuming ideal mixing was within 3−7% of the measured radius, showing consistency in the analysis of the neutron scattering data.

Results

Figure 1 shows SANS measurements of poly(benzyl ether) (PBE) monodendrons of third through sixth generation in *d*-benzene. The data for the sixth generation has been shifted vertically to compensate for its lower concentration (0.37 wt %), necessitated by limited sample availability; otherwise, all of the data are on the original, absolute scale. Figure 2 shows the SANS data for PBE monodendrons of third through fifth generation in *d*-THF. The model fits displayed in both figures are the homogeneous sphere scattering function. These fitting results along with the Guinier radii (fits not shown) are given in Tables 5 and 6. As can be seen, the radii of gyration increase with generation and are larger in *d*-benzene than in *d*-THF. Generally, the Guinier radii agree with those extracted from fitting the entire

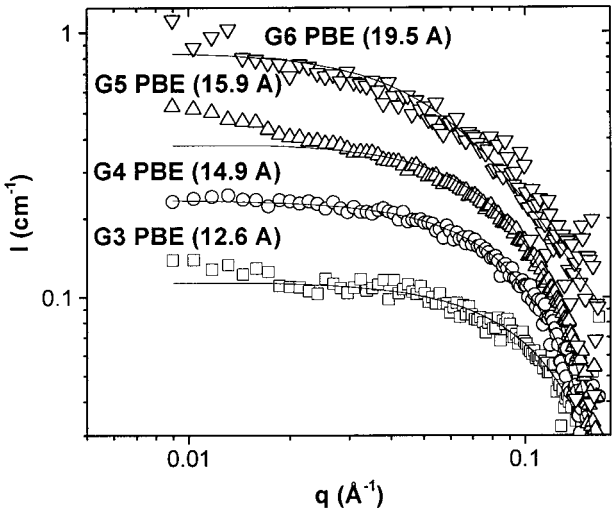

Figure 1. Absolute small-angle neutron scattering spectra for G3 through G6 poly(benzyl ether) dendrons in *d*-benzene. Solid lines represent fits to the sphere form factor.

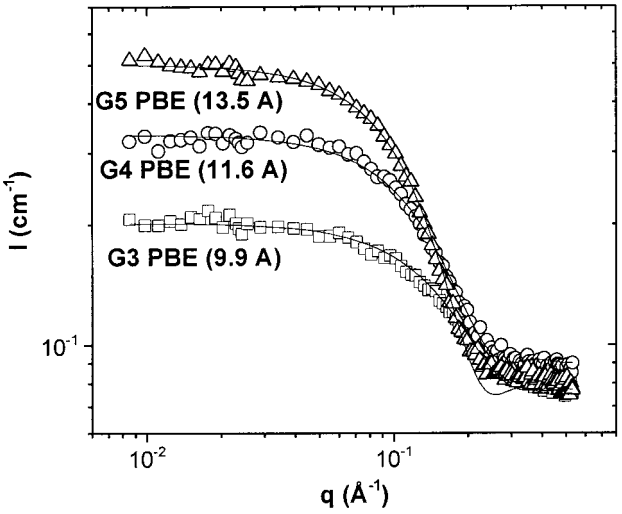

Figure 2. Absolute small-angle neutron scattering spectra for G3 through G5 poly(benzyl ether) dendrons in *d*-THF. Solid lines represent fits to the sphere form factor.

Table 5. SANS Fitting Results for PBE Dendrimers in Deuterated Benzene; R Is the Homogeneous Sphere Radius Derived from the Model

G	R (Å) sphere[a]	R_g (Å) sphere[a]	R_g (Å) Guinier	$I(0)$ (cm^{-1})	mass fraction of solvent	R-square (fit quality)
3	16.3 ± 0.3	12.6 ± 0.2	13.9 ± 0.7	0.115 ± 0.002	0.834	0.922
4	19.3 ± 0.1	14.9 ± 0.1	15.7 ± 0.6	0.235 ±.001	0.795	0.991
5	20.5 ± 0.1	15.9 ± 0.1	18.9 ± 0.8	0.387 ± 0.003	0.692	0.987
6	25.1 ± 0.5	19.5 ± 0.4	21.4 ± 4	0.708 ± 0.014	0.686	0.917

[a] Results of fits of SANS data to the sphere form factor (shown in Figure 1). The radius, R, is the fitting parameter. R_g was calculated from $R_g = \sqrt{(3/5)}R$.

Table 6. SANS Fitting Results for PBE Dendrimers in Deuterated THF; R Is the Homogeneous Sphere Radius

G	R (Å) sphere[a]	R_g (Å) sphere[a]	R_g (Å) Guinier	$I(0)$ (cm^{-1})	mass fraction of solvent	R-square (fit quality)
3	12.8 ± 0.1	9.9 ± 0.1	11.0 ± 0.6	0.125 ± 0.001	0.742	0.981
4	15.0 ± 0.1	11.6 ± 0.1	11.4 ± 0.4	0.243 ± 0.001	0.682	0.995
5	17.4 ± 0.1	13.5 ± 0.1	13.1 ± 0.3	0.425 ± 0.002	0.617	0.997

[a] Results of fits of SANS data to the sphere form factor (shown in Figure 2). The radius, R, is the fitting parameter. R_g was calculated from $R_g = \sqrt{(3/5)}R$.

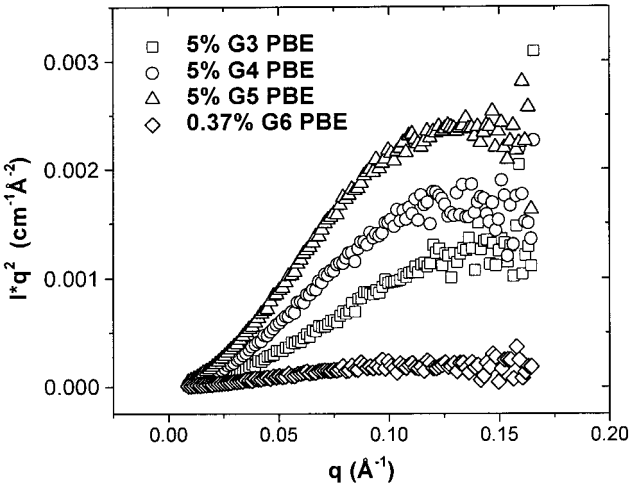

Figure 3. Kratky plot of PBE dendrons in deuterated benzene.

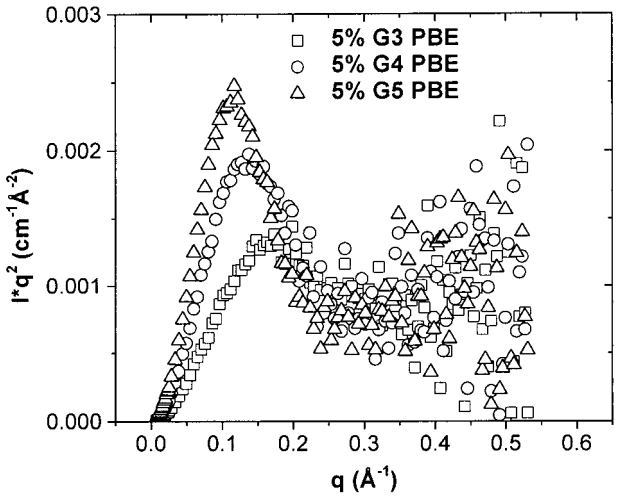

Figure 4. Kratky plot of PBE dendrons in deuterated tetrahydrofuran.

curve; in the following the homogeneous sphere fits will be used for comparison.

Also given in Tables 5 and 6 are estimates of the mass fraction of solvent inside the dendron. These estimates suggest that the amount of solvent within the molecules decreases with generation number, most likely due to increased steric crowding as further generations are added. The increased swelling of the dendrons in *d*-benzene relative to *d*-THF also agrees with the observed larger radii of gyration in *d*-benzene.

Kratky plots, shown in Figures 3 and 4, show behavior typical of branched polymers, although only the data for dendrons in *d*-THF have a q range large enough to fully capture the maximum. Instrument noise and background incoherent scattering precludes distinguishing any higher-order maxima for these lower generation dendrimers. The former Kratky plots qualitatively follow the predictions of Mansfield for low generation number. Thus, the detailed analysis of the SANS data, in terms of both the shape of the curve and analysis of the absolute scattering intensity, justifies the fitting to a homogeneous sphere to first order, in agreement with previous studies.[12,34]

The R_g/R_η ratios given in Table 7 are calculated from the radii of gyration from this work and the intrinsic viscosity measurements of Jeong et al.[26] on the same materials. The ratios for monodendrons in benzene are

Table 7. Summary of Radii (Å) from Our SANS Measurements along with Recently Published Viscosimetric Radii from Intrinsic Viscosity Measurements for Poly(benzyl ether) Monodendrons

	PBE in *d*-benzene			PBE in *d*-THF		
G	R_η	R_g	R_g/R_η	R_η	R_g	R_g/R_η
3	9.8	12.7	1.29	10.4	9.9	0.95
4	14.5	14.9	1.03	14.3	11.6	0.81
5	15.0	15.9	1.06	17.8	13.5	0.76
6	16.5	19.5	1.18			

significantly higher than that observed for the same dendrons in THF or for the PPI dendrimers. Furthermore, the ratio actually begins to increase with increasing generation number, exceeding the value for a Gaussian density distribution (random coil). This may be attributed to solvency effects; benzene has been shown to be a very good solvent for PBE,[26] whereas D_2O is not expected to be as good for PPI. This nonmonatonic behavior (see Figure 5) is in qualitative agreement with the results shown for R_g/R_h for the PAMAM dendrimers in methanol in Table 2.

The PBE dendrons in THF exhibit behavior that more closely resembles the predictions of Mansfield as well as the results for the PPI dendrimers. With increasing generation number, the ratio rapidly tends toward the value for a solid sphere. These results suggest that good solvents can swell dendrimers of higher generation and

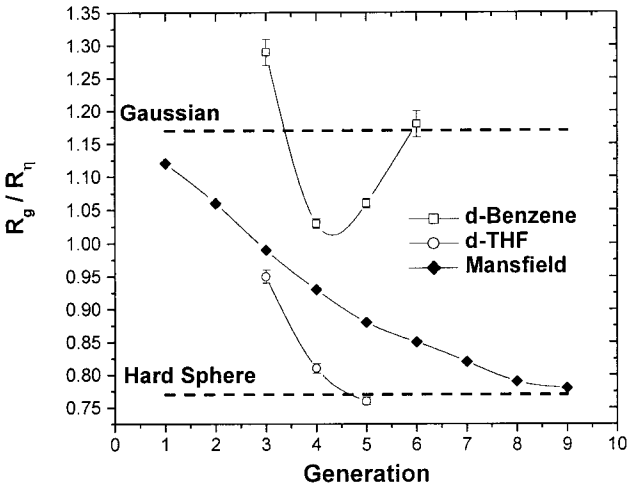

Figure 5. Plot of R_g/R_η vs generation number from the experimental values of this work and the calculations of Mansfield.[11]

open their structure, whereas poorer solvents lead to a densification of the structure with increasing generation number.

It is relevant to consider whether there are any fundamental structural differences evident between monodendrons and full dendrimers in solution. That is, is there a change in the polymer conformation when linked to a multifunctional core? A recently published study by Evmenenko et al. measured the size of a series of PBE dendrimers in both THF and toluene using SANS.[39] The radii of gyration of these full dendrimers are observed to be comparable to that estimated from linking together our monodendrons into the same topology. However, the calculated fraction of solvent within the dendrimer molecule was calculated to be far less (on the order of 25−49 vol % as compared to 65−87 wt %) then what we calculated for the monodendrons. For reference, Bodnar et al.[12] measured values of 44−61 wt % for PPI dendrimers of generation 4−5 in D_2O. This difference between our results and those of Evmenenko et al. cannot be simply explained by the different assumptions made for the bulk polymer density. Also, the effect of solvent quality on R_g is observed to be larger for monodendrons. It is evident that the monodendrons appear to be more swellable then dendrimers, possibly due to decreased steric crowding.

The familiar maximum in the intrinsic viscosity is observed for PBE dendrimers between fourth and fifth generation for both solvents, whereas Mansfield's results show a maximum for the sixth generation. Ganazzoli et al. do not report a maximum in good solvent. Although this shift relative to Mansfield's calculations may be attributable to detailed structural differences in the model vs the experiments (i.e., the use of monodendrons), the comparison helps to distinguish among the theoretical approaches.

Conclusions

A semiquantitative agreement is observed for the ratio R_g/R_η for PBE dendrons in THF and the calculations of Mansfield. However, strong solvency effects are evident in the measured radii of gyration and viscosimetric radii as well as in the ratio R_g/R_η. Similar trends are observed for PPI and PAMAM dendrimers as reported in the literature. Consequently, when comparing simulation and experiment, the thermodynamic interactions of the dendrimer and solvent should be explicitly considered.[19,41] As noted by Mansfield, the assumption of Θ conditions is invalidated by the low molar mass between branch points and strong steric effects due to the highly branched molecular architecture. As shown here, simulations that account for these effects are more successful in predicting the properties of dendrimers, but there remains room for quantitative improvement, especially for good solvents.

Acknowledgment. We gratefully acknowledge careful reviewing of this manuscript. Fruitful conversations with Prof. Mansfield are greatly appreciated. SANS measurements were performed at the National Institute of Standards and Technology. This material is based on activities supported by the NSF under DMR-9423101. Funding from DuPont is gratefully acknowledged by N.J.W. and B.M.T. as well as insightful discussions with Dr. Young Kim of DuPont.

References and Notes

(1) Bosman, A. W.; Janssen, H. M.; Meijer, E. W. *Chem. Rev.* **1999**, *99*, 1655.
(2) Hawker, C. J. *Curr. Opin. Colloid Interface Sci.* **1999**, *4*, 117.
(3) Newkome, G. R.; He, E.; Moorefield, C. N. *Chem. Rev.* **1999**, *99*, 1689.
(4) deGennes, P. G.; Hervet, H. *J. Phys., Lett.* **1983**, *44*, L351.
(5) Lescanec, R. L.; Muthukumar, M. *Macromolecules* **1990**, *23*, 2280.
(6) Cagin, T.; Wang, G. F.; Breen, M. R.; Goddard, W. A. *Nanotechnology* **2000**, *11*, 77.
(7) Ganazzoli, F.; La Ferla, R.; Terragni, G. *Macromolecules* **2000**, *33*, 6611.
(8) La Ferla, R. *J. Chem. Phys.* **1997**, *106*, 688.
(9) Lue, L. *Macromolecules* **2000**, *33*, 2266.
(10) Lyulin, A. V.; Davis, G. R.; Adolf, D. B. *Macromolecules* **2000**, *33*, 3294.
(11) Mansfield, M. L. *Macromolecules* **2000**, *33*, 8043.
(12) Bodnar, I.; Silva, A. D.; Deitcher, R. W.; Weisman, N. E.; Kim, Y. H.; Wagner, N. J. *J. Polym. Sci., Part B: Polym. Phys.* **2000**, *38*, 857.
(13) Bodnar, I.; Silva, A. D.; Kim, Y. H.; Wagner, N. J. *J. Polym. Sci., Part B: Polym. Phys.* **2000**, *38*, 874.
(14) Choi, S.; Briber, R. M.; Bauer, B. J.; Liu, D.-W.; Gauther, M. *Macromolecules* **2000**, *33*, 6495.
(15) Poetschke, D.; Ballauff, M.; Lindner, P.; Fischer, M.; Voegtle, F. *Macromolecules* **1999**, *32*, 4079.
(16) Poetschke, D.; Ballauff, M.; Lindner, P.; Fischer, M.; Voegtle, F. *Macromol. Chem. Phys.* **2000**, *201*, 330.
(17) Ramzi, A.; Scherrenberg, R.; Brackman, J.; Joosten, J.; Mortensen, K. *Macromolecules* **1998**, *31*, 1621.
(18) Scherrenberg, R.; Coussens, B.; van Vliet, P.; Edouard, G.; Brackman, J.; de Brabander, E. *Macromolecules* **1998**, *31*, 456.
(19) Trollsas, M.; Atthof, B.; Würsch, A.; Hedrick, J. L.; Pople, J. A.; Gast, A. P. *Macromolecules* **2000**, *33*, 6423.
(20) Tropp, A.; Bauer, B. J.; Klimash, J. W.; Spindler, R.; Tomalia, D. A.; Amis, E. J. *Macromolecules* **1999**, *32*, 7226.
(21) Tropp, A.; Bauer, B. J.; Prosa, T. J.; Scherrenberg, R.; Amis, E. J. *Macromolecules* **1999**, *32*, 8923.
(22) Sendijarevic, I.; McHugh, A. J. *Macromolecules*, in press.
(23) Uppuluri, S.; Morrison, F. A.; Dvornic, P. R. *Macromolecules* **1999**, *32*, 2.
(24) Hong, Y.; Cooper-White, J. J.; Mackay, M. E.; Hawker, C. J.; Malmström, E.; Rehnberg, N. *J. Rheol.* **1999**, *43*, 781.
(25) Hawker, C. J.; Farrington, P. J.; Mackay, M. E.; Wooley, K. L.; Fréchet, J. M. J. *J. Am. Chem. Soc.* **1995**, *117*, 4409.
(26) Jeong, M.; Mackay, M. E.; Vestberg, R.; Hawker, C. J. *Macromolecules* **2001**, *34*, 4927.
(27) Farrington, P. J.; Craig, J. H.; Fréchet, J. M. J.; Mackay, M. E. *Macromolecules* **1998**, *31*, 5043.
(28) Schmidt, M.; Burchard, W. *Macromolecules* **1981**, *14*, 210.
(29) Flory, P. J. *Principles of Polymer Chemistry;* Cornell University Press: Ithaca, NY, 1953.

(30) Burchard, W. Solution Properties of Branched Molecules. In *Advances in Polymer Science*; Springer-Verlag: Berlin, 1999; p 113.
(31) Mourey, T. H.; Turner, S. R.; Rubenstein, M.; Frechet, J. M. J.; Hawker, C. J.; Wooley, K. L. *Macromolecules* **1992**, *25*, 2401.
(32) Cai, C.; Chen, Z. Y. *Macromolecules* **1998**, *31*, 6393.
(33) Rietveld, I. B.; Bedeaux, D. *Macromolecules* **2000**, *33***,** 7912.
(34) Prosa, T. J.; Bauer, B. J.; Amis, E. J.; Tomalia, D. A.; Scherrenberg, R. *J. Polym. Sci., Part B: Polym. Phys.* **1997**, *35***,** 2913.
(35) Mansfield, M. L.; Klushin, L. I. *J. Phys. Chem.* **1992**, *96*, 3994.
(36) Stechemesser, S.; Eimer, W. *Macromolecules* **1997**, *30*, 2204.
(37) Hubbard, J. B.; Douglas, J. F. *Phys. Rev. E* **1993**, *47***,** R2983.
(38) Hawker, C. J.; Frechet, J. M. J. *J. Am. Chem. Soc.* **1990**, *112*, 7638.
(39) Evmenenko, G.; Bauer, B. J.; Kleppinger, R.; Forier, B.; Dehaen, W.; Amis, E. J.; Mischenko, N.; Reynaers, H. *Macromol. Chem. Phys.* **2001**, *202***,** 891.
(40) Hay, G.; Mackay, M. E.; Hawker, C. J. *J. Polym. Sci., Part B: Polym. Phys.* **2001**, *39***,** 1766.
(41) Welch, P. M.; Mathias, L. J.; Lescanec, R. L. *Polym. Prepr.* **1996**, *37***,** 250.
(42) Rietveld, I. B.; Smit, J. A. M. *Macromolecules* **1999**, *32*, 4608.

MA011265G